Vol. 81 No. 1 pp. 68–80 ACTA GEOLOGICA SINICA Feb. 2007

Three Stages of Zircon Growth in Magmatic Rocks from the Pingtan Complex, Eastern China

WANG Xiang[1, 2, *], W. L. GRIFFIN[2, 3], S. Y. O'REILLY[2] and LI Wuxian[1]
1 *State Key Laboratory for Mineral Deposit Research, Department of Earth Sciences, Nanjing University, Nanjing, Jiangsu 210093, China*
2 *GEMOC ARC National Key Center, Department of Earth and Planetary Sciences, Macquarie University, NSW 2109, Australia*
3 *CSIRO Exploration and Mining, North Ryde, NSW 2113, Australia*

Abstract: Morphological and chemical studies on zircon grains from gabbro and granite of the Pingtan magmatic complex, Fujian Province, eastern China, show that there are three stages of zircon growth. The early stage of zircon growth is characterized by colorlessness, high transparence and birefringence, low and dispersive I_{pr} and I_{py}, weak and homogeneous BSE brightness, lower Hf content and depletion of U, Th and Y; the middle stage is characterized by abruptly increasing I_{py}, progressively strong and sectoral-zoning BSE brightness, higher Hf content and enrichment of U, Th and Y with Th/U > 1; the late stage of growth is characterized by brownish color, poor transparence, low birefringence, highest I_{pr} and I_{py}, middle and oscillatorily-zoning BSE brightness, highest contents of Hf, U and Y with Th/U < 1. The stages are considered to be formed in a deep magma chamber, ascent passage and emplacement site, respectively. Due to the more or less long residual time of the magma chamber, the difference in age between the early and late stages of zircon might be great enough to be distinguished, which can be attributed to tectonic constraint for the magmatism.

Key words: zircon, three stages of crystal growth, typology, trace element, magmatic rock

1 Introduction

Zircon is a ubiquitous accessory mineral in most igneous rocks, and its morphology and chemistry often record its primary crystallization history due to its stability in many crustal process. Therefore, zircons have been regarded as an important subject in petrological, geochemical and geochronological studies.

According to classical ideas, small and euhedral zircon, as accessory minerals, crystallized shortly in a cooling magma. For example, zircon has been regarded as forming in residual basaltic magma as a late crystallization product since the magma would be saturated in ZrO_2 and SiO_2 only after fractional crystallization of the majority of rock-forming minerals (Poldervaart, 1956; Konzett et al., 1998; Vavra et al., 1999) whereas zircon in granitic magma, as a liquidus phase, crystallized before any of the other minerals (Poldervaart, 1956; Alper and Poldervaart, 1957; Larsen and Poldervaart, 1957). However, recent studies reveal that there exist early-crystallized zircons in basaltic magma (Ashwal et al., 1999; Belousova et al., 2002), and late-crystallized zircons (i.e., from the residual magma) in granitic magma (Speer, 1982; Rubin et al., 1989; Pupin, 1992; Benisek and Finger, 1993; Caironi et al., 2000). So it is now considered that zircons crystallize continually in a cooling magma (Silver and Deutsch, 1963; Veniale et al., 1968; Yeliseyeva et al., 1974; Speer, 1982). Especially, this is emphasized by the fact that zircon may be internally heterogeneous showing two or three broad growth bands of clearly different brightness in a backscattered electron (BSE) image (Broska et al., 1990; Benisek and Finger, 1993; Ansdell and Kyser, 1991; Gebauer and Grunenfelder, 1979; Schärer et al., 1994; Connelly, 2000; Caironi et al., 2000; Charlier and Zellmer, 2000; Wang and Kienast, 1999; Wang, X. et al., 2002), significantly indicating a multi-stage growth history for the zircons in some magmatic rocks. On the other hand, geochronological data from in situ or single grain U-Pb dating methods show that zircon grains from the same population of certain magmatic rocks have more than one age (Keay et al., 1999; Vavra et al., 1999; Wilde et al., 2003). If the latter could be

* Corresponding author. E-mail: xwang@nju.edu.cn.

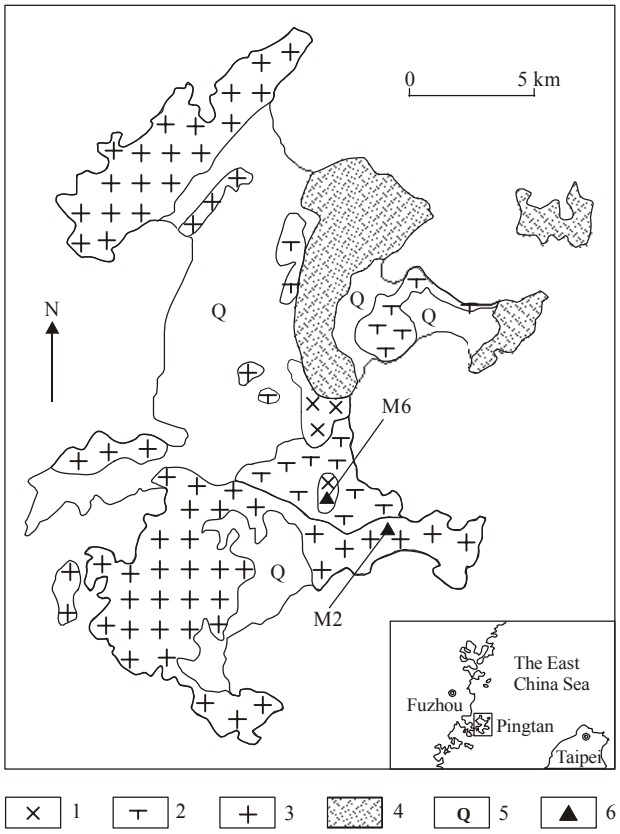

Fig. 1. Geological sketch map of the Pingtan magmatic complex, Fujian Province, eastern China.
1. Gabbro; 2. Granodiorite; 3. Granite; 4. Volcanic rocks; 5. Quaternary; 6. Sampling locality.

confirmed this would affect our traditional understanding of geochronology, petrology and tectonics.

This paper reports a detailed study of magmatic zircon in gabbro and granite from the Pingtan magmatic complex, eastern China. Based on observations of the external morphology, internal structure and chemical analysis we can distinguish three stages of zircon growth in both the gabbro and the granite. We then determine their crystallization environment during the formation of igneous rocks, and discuss the implications for petrogenesis of magmatic rocks.

2 Samples and Analytical Techniques

Magmatic rock samples used in this study were collected from the Pingtan magmatic complex located on Pingtan Island in Fujian Province, eastern China (Fig. 1). The gabbro sample (M6) was collected from a gabbroic stock located near the central part of the complex (119°46′45″ E and 25°29′50″ N). It consists of plagioclase, hornblende and pyroxene with minor amounts of magnetite and quartz. The granite sample (M2) was collected from the dominant part of the complex (119°44′47″ E and 25°25′36″ N). It consists of quartz, K-feldspar, plagioclase and minor amounts of biotite. The Pingtan magmatic complex is considered to be the product of magmatic activity induced by the subduction of the Pacific Plate beneath the Eurasian continent in the late Mesozoic time (Dong et al., 1997; Xu et al., 1999).

Each rock sample, weighing 2 kg, was crushed and sieved to less than 0.2 mm. Zircon grains were separated according to magnetic properties and density, and finally selected by hand picking. They were embedded in epoxy and polished down to expose the grain centers.

According to the quantitative description method of zircon morphology (Wang, 1998), three typological indices (i.e., I_{pr}, I_{py} and I_{el}) of all grains were measured under an ordinary microscope, and were plotted to determine the distribution of their external morphology. Then, using a Camebax SX50 electron microprobe at GEMOC, Macquarie University (Sydney, Australia), the internal structure of the zircons was observed on sections of single grains by means of BSE imaging. A BSE image reflects differences in the mean atomic number of the zircon composition.

The same microprobe was used for analysis of major elements (Zr and Si) and substituted elements (Hf, U, Th and Y) in the zircon. Analytical conditions were 15 kV acceleration voltage and 20 nA beam current. The spatial resolution of the electron microprobe was about 2 μm. Counting times were 20 seconds for Zr, Si and Hf, and 60 s for U, Th and Y. Standards were natural zircon for Zr and Si, Hf metal for Hf, and synthetic oxides for U, Th and Y. The precision of the analyses, based on counting statistics, is ca. 0.03 wt% oxide (1σ) for all of these elements.

3 Results

3.1 External morphology and internal structure

Under the microscope all zircon grains from both the gabbro and the granite were characterized by common features of magmatic origin such as euhedral and prismatic shape, invariable size, primary growth zoning, and melt inclusion, etc. However, according to their optical properties, each population of zircons from both the gabbro and the granite can be divided into two stages: early stage of zircon (ESZ) and late stage of zircon (LSZ). ESZ is colorless with high transparence and birefringence, acute shape (i.e., importance of the {211} faces relative to the {101} faces), high in grain quantity (Fig. 2a–c, 2f), and LSZ is light yellow-brown with low transparence and birefringence due to metamictization, stubby shape (i.e., importance of the {101} faces relative to the {211} faces), and low in grain quantity (Fig. 2d, 2e, 2h–k). Within many grains ESZ and LSZ may show typical core-rim structure, i.

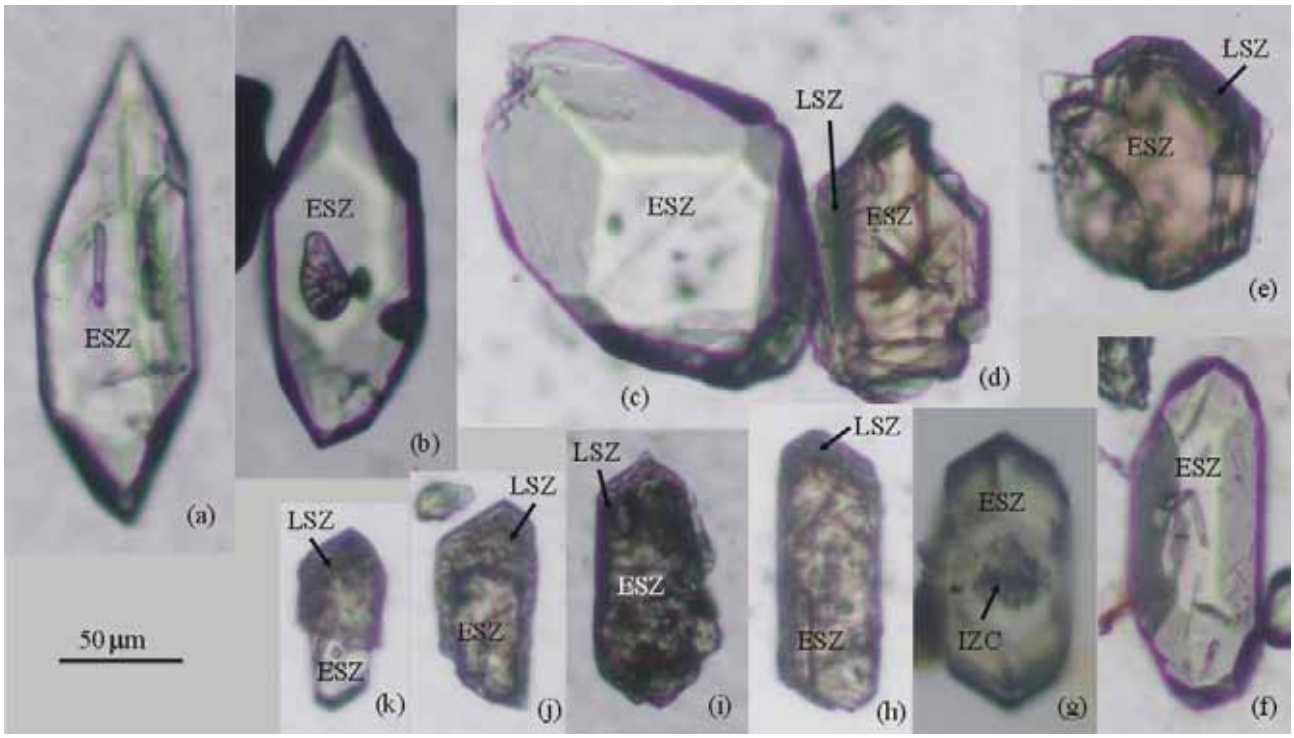

Fig. 2. Optical photomicrographs (scale bars = 50 μm) of ESZ, LSZ and IZC (inherited zircon core) in the gabbro (a–e) and the granite (f–k) from the Pingtan magmatic complex.

Table 1 Averages of typological indices for the early stage of zircon (ESZ) and the late stage of zircon (LSZ) in the gabbro and the granite from the Pingtan magmatic complex

Rock	Gabbro		Granite	
Zircon	ESZ	LSZ	ESZ	LSZ
	n = 25	n = 10	n = 24	n = 20
I_{pr}	0.59	0.58	0.48	0.80
I_{py}	0.53	0.99	0.77	1.00
I_{el}	0.52	0.47	0.58	0.68

e., ESZ is overgrown by LSZ (Fig. 2d, 2e, 2h–k).

Typologically, ESZ and LSZ in both the gabbro and the granite samples from the Pingtan magmatic complex are significantly distinct as follows:

(1) ESZ is characterized by larger ranges of I_{py} with a smaller mean I_{py} relative LSZ (Table 1). For example, in the gabbro I_{py} of ESZ ranges between 0.14 and 0.82 with an average of 0.53, whereas I_{py} of LSZ between 0.94 and 1.00 with an average of 0.99 (Fig. 3a);

(2) ESZ has a smaller mean I_{pr} relative to LSZ (Table 1), but the variation of I_{pr} may be large for both ESZ and LSZ. For example, in the granite, ESZ has a mean I_{pr} of 0.48 with I_{pr} ranging between 0.20 and 0.72, whereas LSZ has a mean I_{pr} of 0.80 with I_{pr} ranging between 0.45 and 1.00 (Fig. 3b);

(3) But, ESZ and LSZ have very similar values of I_{el} (Table 1). Since LSZ appears essentially in form of the stubby {101} shape relative to the acute {211} shape of ESZ, I_{el} may decrease slightly from ESZ to LSZ as LSZ occurs as a thin shell overgrowth on ESZ in the Pingtan gabbro (Fig. 2d and 2e), and may also increase slightly from ESZ to LSZ as LSZ is very developed with preferential overgrowth at both ends of the prismatic crystals in the Pingtan granite (Fig. 2h and 2j).

On BSE images, it is clearer that there are two stages of zircon in both the Pingtan gabbro and the granite. ESZ is characterized by weak (dark) and homogeneous BSE brightness without any growth zoning (Fig. 4a – f), and LSZ is characterized by strong (light) and oscillatory-zoned BSE brightness (Fig. 4a–e). Particularly, a middle stage of zircon (MSZ) was observed as a thin overgrowth zone between ESZ and LSZ, which is characterized by progressive zoning and sector zoning (Fig. 4a–f), reflected by increasing the BSE brightness from the inner to the outer zone with the difference in BSE brightness between the prismatic and the pyramidal parts within a same zone. Because MSZ is poorly developed, and does not occur often as single grains, it has not been observed under the microscope.

In addition, some inherited zircons have been found as cores (labelled as IZC) within ESZ from the Pingtan granite (Fig. 2g and Fig. 4f). They are characterized by irregular, eroded ovoid forms with dentate outlines, indicating that they were in disequilibrium with the host magma. Heterogeneous BSE brightness and many cavities within them suggest that they had undergone metamictization

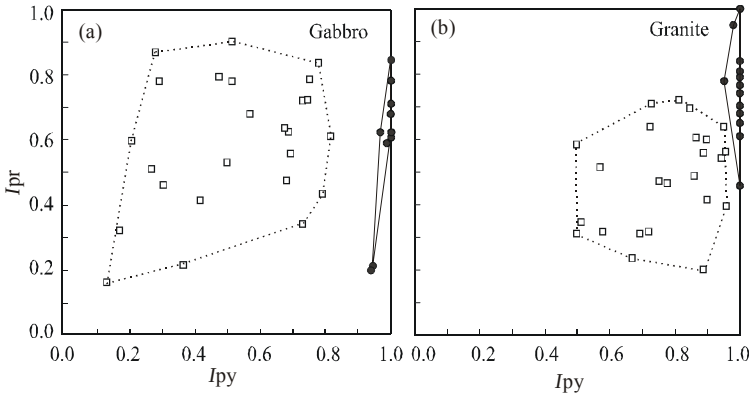

Fig. 3. Plot of I_{pr} versus I_{py} of ESZ (open squares) and LSZ (closed circles) in the gabbro (a) and the granite (b) from the Pingtan magmatic complex.

before they were enclosed by the host magma. Thus, the cores are thought to have been inherited from the protolith during partial melting in the crust.

3.2 Chemical composition

Many cationic elements may substitute for Zr^{4+} in zircon (Belousova et al., 2002). They can be divided into two groups based on crystal chemistry: one comprises completely isomorphous cations such as Hf^{4+}; its slightly smaller ionic radius allows it to enter the zircon lattice and form a complete solid solution. The other group includes incompletely isomorphous cations such as U^{4+}, Th^{4+}, Y^{3+}, etc.; their much larger ionic radii only allows limited solid solution (Wang and Li, 2002). The electron microprobe analysis (Table 2) shows that the three stages of zircon differ strongly in content of these two groups of elements.

(1) ESZ is characterized by very low contents of the incompletely isomorphous elements, which are below 0.30 and 0.50 wt % (UO_2+ThO_2+Y_2O_3) for the gabbro and the granite, respectively (Fig. 5a, 5b). Especially, the contents of UO_2 or ThO_2 typically are below the electron-microprobe detection limits (Fig. 5c, 5d). The contents of HfO_2 in ESZ are relatively low but very variable. For example, the contents of HfO_2 range from 0.83 to 1.31 wt% with a mean content of 1.08 wt% for the gabbro, and from 1.21 to 1.83 wt% with a mean content of 1.48 wt% for the granite (Fig. 5a, 5b).

(2) MSZ contains significant amounts of incompletely isomorphous elements with mean contents of 0.99 and 1.89 wt% (UO_2+ThO_2+Y_2O_3) for the gabbro and the granite, respectively (Fig. 5a, 5b). However, the most significant character for MSZ is that the content of ThO_2 is greater than that of UO_2 with mean ThO_2/UO_2 ratios of 2.0 and 2.4 for the gabbro and the granite, respectively (Fig. 5c, 5d). The contents of HfO_2 in MSZ are higher than those in ESZ for the gabbro with a mean content of 1.44 wt%, and lower than those in ESZ for the granite with a mean content of 1.27 wt% (Fig. 5a, 5b). This difference may be attributed to differences in crystallization order of the MSZ relative to the main rock-forming minerals between the gabbro and the

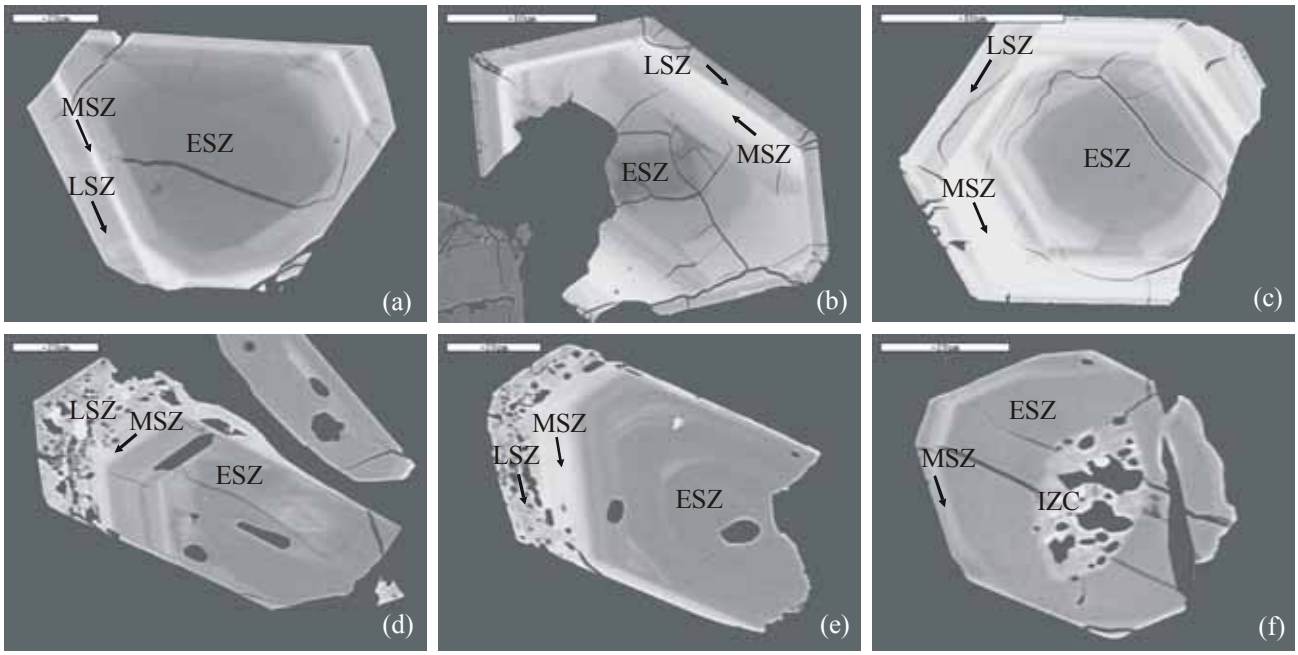

Fig. 4. BSE images of ESZ, MSZ, LSZ and IZC (inherited zircon core) in the gabbro (a, b and c) and the granite (d, e and f) from the Pingtan magmatic complex.

Table 2 Microprobe analyses of zircons from the gabbro (M6) and the granite (M2) of the Pingtan magmatic complex

Grain	M6-1			M6-2	M6-3							
Stage	ESZ	MSZ	LSZ	ESZ	ESZ	ESZ	ESZ	ESZ	ESZ	ESZ	ESZ	ESZ
HfO_2	1.21	1.58	1.74	0.98	1.17	1.26	1.11	1.23	1.04	1.05	1.16	1.29
UO_2	0.05	0.17	1.08	0.07	b.d.	0.06	0.07	b.d.	b.d.	b.d.	0.09	0.04
ThO_2	0.07	0.20	0.27	b.d.	0.05	0.04	0.03	0.03	b.d.	b.d.	0.06	0.04
Y_2O_3	b.d.	0.16	0.19	0.06	0.06	0.08	0.12	b.d.	b.d.	0.07	0.04	0.04
ZrO_2	66.23	64.40	64.20	66.39	65.87	66.65	66.48	66.86	66.20	65.81	67.01	66.11
SiO_2	32.93	32.23	32.29	33.43	33.48	33.39	33.36	33.47	33.42	33.32	33.28	33.03
Total	100.49	98.74	99.76	100.94	100.66	101.48	101.17	101.58	100.70	100.25	101.64	100.55

Grain	M6-3					M6-4			M6-5			
Stage	ESZ	ESZ	ESZ	MSZ	MSZ	ESZ	ESZ	MSZ	ESZ	MSZ	MSZ	MSZ
HfO_2	1.17	1.16	1.31	1.45	1.26	1.21	1.25	1.48	1.10	1.42	1.34	1.55
UO_2	0.09	0.03	0.12	0.06	0.18	0.03	0.08	0.40	b.d.	0.20	0.34	0.52
ThO_2	b.d.	b.d.	0.12	0.17	0.28	0.03	0.11	0.71	b.d.	0.26	0.99	1.27
Y_2O_3	b.d.	b.d.	0.07	0.04	0.23	b.d.	0.09	0.31	0.08	0.39	0.27	0.27
ZrO_2	66.87	65.35	66.56	66.80	66.33	66.18	67.34	64.53	66.16	65.56	64.69	63.79
SiO_2	33.36	33.40	33.39	33.45	33.42	33.53	33.36	33.19	33.58	33.49	33.22	32.91
Total	101.50	99.98	101.57	101.96	101.69	100.99	102.24	100.62	100.94	101.33	100.85	100.31

Grain	M6-5	M6-6		M6-7		M6-8			M6-9		M6-10	
Stage	LSZ	ESZ	ESZ	ESZ	ESZ	ESZ	ESZ	MSZ	ESZ	MSZ	ESZ	LSZ
HfO_2	1.84	0.97	0.95	1.13	0.86	1.07	1.06	1.51	0.83	1.33	1.01	1.74
UO_2	0.46	0.05	b.d.	0.10	0.04	b.d.	0.07	0.32	0.03	0.16	0.03	0.86
ThO_2	0.07	b.d.	b.d.	0.06	0.07	b.d.	b.d.	0.38	b.d.	0.34	0.03	0.25
Y_2O_3	0.12	0.04	0.09	0.03	b.d.	0.10	b.d.	0.13	b.d.	0.22	0.04	0.05
ZrO_2	64.75	66.85	66.81	66.36	65.82	67.04	67.22	65.53	65.83	65.37	66.74	64.37
SiO_2	33.49	33.86	33.65	33.58	33.47	33.63	33.72	33.40	33.64	33.44	33.45	33.15
Total	100.73	101.79	101.49	101.25	100.26	101.85	102.08	101.27	100.34	100.86	101.29	100.41

Grain	M6-10	M6-11			M6-12		M2-1					
Stage	LSZ	ESZ	ESZ	ESZ	ESZ	ESZ	ESZ	ESZ	ESZ	ESZ	MSZ	ESZ
HfO_2	1.67	0.91	0.86	1.01	0.88	0.93	1.48	1.52	1.26	1.60	1.47	1.83
UO_2	0.56	b.d.	0.04	b.d.	b.d.	b.d.	b.d.	b.d.	b.d.	0.05	0.38	0.09
ThO_2	0.16	b.d.	0.03	b.d.	0.05	0.11	0.08	0.03	0.04	b.d.	0.61	b.d.
Y_2O_3	0.23	0.09	0.14	b.d.	b.d.	0.09	0.21	0.15	0.26	0.25	1.11	0.18
ZrO_2	63.96	66.89	66.50	66.87	66.48	66.53	65.34	64.88	65.73	65.10	62.45	65.68
SiO_2	33.26	33.65	33.60	33.58	33.42	33.53	32.57	32.08	32.56	32.71	31.94	32.84
Total	99.85	101.55	101.17	101.49	100.83	101.20	99.68	98.65	99.85	99.72	97.96	100.62

Grain	M2-1	M2-2	M2-3	M2-4	M2-5						M2-6	M2-7
Stage	ESZ	ESZ	LSZ	ESZ	ESZ	ESZ	ESZ	ESZ	ESZ	ESZ	ESZ	MSZ
HfO_2	1.25	1.51	1.84	1.44	1.35	1.74	1.67	1.51	1.44	1.54	1.21	1.14
UO_2	b.d.	b.d.	0.89	b.d.	0.07	0.03	0.05	b.d.	0.06	0.07	b.d.	0.15
ThO_2	b.d.	0.05	0.36	b.d.	0.05	b.d.	b.d.	b.d.	b.d.	b.d.	b.d.	0.28
Y_2O_3	0.24	0.04	1.00	0.28	0.37	0.15	0.09	0.08	0.09	0.07	0.10	1.08
ZrO_2	64.33	65.48	62.02	65.30	66.30	64.74	65.50	65.59	65.74	65.04	65.41	65.11
SiO_2	32.59	32.47	31.59	32.54	32.52	33.16	32.71	32.57	32.65	32.86	32.47	32.08
Total	98.42	99.55	97.70	99.58	100.66	99.84	100.01	99.78	99.99	99.58	99.19	99.83

Grain	M2-7		M2-8				M2-9		M2-10		M2-11
Stage	MSZ	LSZ	ESZ	ESZ	ESZ	LSZ	ESZ	ESZ	ESZ	LSZ	ESZ
HfO_2	1.21	1.70	1.39	1.48	1.58	1.84	1.32	1.58	1.33	1.87	1.54
UO_2	0.24	0.20	b.d.	b.d.	0.13	0.62	b.d.	b.d.	0.04	0.74	0.06
ThO_2	0.94	0.19	b.d.	b.d.	0.14	0.58	b.d.	b.d.	0.04	0.40	0.08
Y_2O_3	0.90	1.01	0.06	0.10	0.24	1.49	0.05	0.03	0.14	1.15	0.14
ZrO_2	63.14	62.76	66.06	66.26	64.60	63.05	66.45	65.79	65.88	61.62	66.16
SiO_2	31.94	32.02	32.34	32.56	32.25	31.25	32.40	32.46	32.47	31.54	32.29
Total	98.37	97.88	99.85	100.40	98.93	98.82	100.21	99.85	99.89	97.33	100.27

b.d. = below detection.

granite (see discussion below).

(3) LSZ is characterized by slightly higher contents of the incompletely isomorphous elements than those in MSZ, with mean contents of 1.07 and 2.16 wt % (UO_2+ThO_2+Y_2O_3) for the gabbro and the granite, respectively (Fig. 5a, 5b). However, the content of ThO_2 is obviously smaller than that of UO_2 with mean ThO_2/UO_2 ratios of 0.25 and 0.62 for the gabbro and the granite, respectively (Fig. 5c, 5d). The contents of HfO_2 in LSZ are always greater than those in MSZ with mean contents of 1.75 and 1.81 wt% for the gabbro and the granite, respectively (Fig. 5a, 5b).

Published data generally show that zircon in relatively felsic rocks exhibits increase of Hf in overgrowths, usually accompanied by increasing U and Y (Pupin, 1992; Halden et al., 1993; Benisek and Finger, 1993; Wang and Kienast, 1999; Wang, X. et al., 2002).

In conclusion, based on observation of internal structure and the analysis of chemical composition, the zircon crystallization in both the gabbro and the granite from the Pingtan magmatic complex can be divided into three stages, which are probably related to three different environments during the consolidation of the host magma.

4 Discussion

4.1 Magmatic nature of the three stages of zircon

Observations of shape and structure, and chemical analyses show that the zircon populations in both the gabbro and the granite from the Pingtan magmatic complex contain three stages of zircon: ESZ, MSZ and LSZ.

The question then arises whether the three stages of zircon formed during a single magmatic activity. In order to understand their crystallization during a magmatic process, we have to prove firstly that ESZ did not occur before the magmatic activity as relict cores, and secondly that LSZ did not form after the magmatic activity as subsequent hydrothermal overgrowth. Several lines of evidence are relevant:

(1) It can be observed that ESZ was overgrown continuously by MSZ, MSZ was overgrown continuously by LSZ, and sometimes three stages of zircon occur together within a single grain in the form of the growth zones, as shown on many BSE images (Fig. 3a–e). The contours between two of the three stages of zircon are generally euhedral, i.e., the internal phase has not been resorbed significantly. This indicates that the time interval between two different growth zones was not too long, and thus they can be considered as products of a single magmatism.

(2) There are some consecutive evolutions from ESZ via MSZ to LSZ in both the gabbro and the granite: increasing and converging of I_{pr} and I_{py} on the typological side (Fig. 3), and increasing and dispersing of contents of trace elements (Hf, U, Th, and Y) on the chemical side (Fig. 5). In fact, these trends may be interpreted as controlled by change in thermodynamical environments during a single plutonic magmatism (see below).

(3) Detrital grains of zircon have been found in the Pingtan granite, which are typically characterized by rounded shape and poor transparence due to external abrasion and internal metamictization (Fig. 2g and Fig. 4f). These detrital grains of zircon are exclusively included within ESZ, indicating that ESZ itself was not inherited from the source rocks, but was newly crystallized during the granitic magmatism. On the other hand, ESZ is not only euhedral, colorless and transparent in both the gabbro and the granite from the Pingtan magmatic complex, but also is high whether in grain quantity within a zircon population or in volume within zircon grains, so that it is hard to consider this as an inherited origin. In the literature, this type of early stage of zircon with late overgrowth rims is often reported as of magmatic origin (Zartman and Hermes, 1987; Williams, 1992; Corfu, 1996; Nasdala et al., 1999).

(4) LSZ in both the gabbro and the granite from the Pingtan magmatic complex are basically included within the primary rock-forming minerals (biotite, plagioclase, K-feldspar, quartz, etc.). Their enrichment in U and Th results in the occurrence of radioactive aureoles within the host minerals (especially in biotite). On the other hand, the unaltered mineralogy of these rocks eliminates the possibility that LSZ was formed during subsequent hydrothermal alteration.

In the literature many grains of zircon are often internally heterogeneous and showed two or three growth bands revealed by distinct brightnesses on BSE images (Ansdell and Kyser, 1991; Benisek and Finger, 1993), such bands indicating a consecutive crystallization of zircon from a single magma with sharp changes in their crystallization environments (Gebauer and Grunenfelder, 1979; Schärer et al., 1994; Connelly, 2000; Wang and Kienast, 1999; Wang, X. et al., 2002). Morphologically, crystal growth begins with a euhedral nucleus with the {101} and the {211} pyramid faces and the {100} prism faces, and finishes with an oscillatory zoned rim with the only {101} faces (Paterson et al., 1992; Vavra, 1994; Nemchin and Pidgeon, 1997; Pupin, 2000; Charlier and Zellmer, 2000); Chemically, the early generation of zircon appears to be homogeneous with low Hf, U and Th, but the later added zircon is rich in these trace elements (Paterson et al., 1992; Vavra, 1994; Guo et al., 1996; Elburg, 1996; Pupin, 2000). Especially, MSZ has also been found as inner rims between the inner part and the outer rim, characterized by remarkable trace-element enrichments in Hf, U and Th

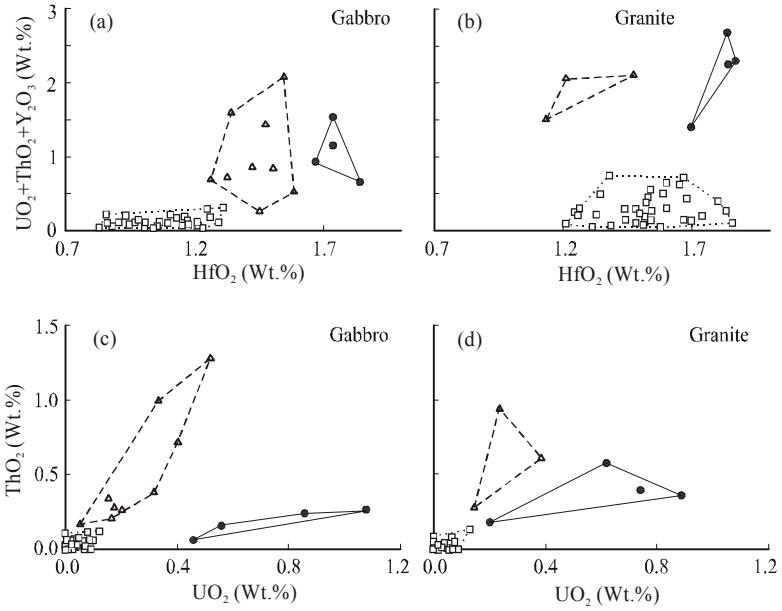

Fig. 5. Plot of HfO_2 (wt%) vs. $UO_2+ThO_2+Y_2O_3$ (wt%) and UO_2 (wt%) vs. ThO_2 (wt%) for ESZ (open squares), MSZ (open triangles) and LSZ (closed circles) in the gabbro (a and c: gabbro) and the granite (b and d: granite) from the Pingtan magmatic complex.

(Broska et al., 1990; Pidgeon and Compston, 1992; Nemchin and Pidgeon, 1997; Poitrasson et al., 1998; Wang and Kienast, 1999). The above phenomena are highly consistent with the morphological and chemical characters of the three stages of zircon, which are considered in this paper to be formed during a single magmatism. In fact, many crystals of zircon from magmatic rocks display no distinction in ages between the inner part and the outer rims, proving convincingly that all these components were formed, resorbed and overgrown during the same short-lived magmatic event (Roddick and Bevier, 1995; Elburg, 1996; Corfu, 1996; Nasdala et al., 1999; Zeck and Whitehouse, 2002).

4.2 Crystallization environment of the three stages of zircon

Although MSZ within magmatic zircon is often poorly developed, its specific occurrence between ESZ and LSZ plays an important role in determining the crystallization environment of the three stages of zircon formed from a single magma. In fact, MSZ shows some significant characters, as follows:

(1) The structure of MSZ is characterized by progressive zoning and sector zoning, which commonly indicate a very high growth rate of crystals relative to diffusion rate of elements in the melt (Burton et al., 1953; Bryan, 1972).

(2) The chemistry of MSZ is characterized by very high contents of U, Th and Y, and linear variation between U and Th with Th/U >1. The relatively faster growth rate of crystals allows the constituent elements with larger ionic radii (e.g. Y, U and Th) to enter the zircon lattice (Carpéna et al., 1987; Vavra et al., 1999; Wang and Kienast, 1999). Vavra et al. (1999) concluded that higher Th/U ratios in zircons may be the result of a kinetically fast and chemically less selective continuous growth mechanism, making the Th/U ratio in the crystal more similar to that of the environment where the ratio is commonly larger than 1 (Faure, 1977).

(3) MSZ is generally poorly developed, showing its very short time of crystallization in spite of its faster growth rate.

The above features of MSZ suggest that it was formed under non-equilibrium conditions, which can be caused by high undercooling, resulting from a rapid ascent of the host magma. In fact, MSZ is better developed in the gabbro than in the granite of the Pingtan magmatic complex, and thus there is a negative correlation between the development of MSZ and the relative volumes of the host magmas, or a positive correlation between the development of MSZ and the magma temperature of the host magmas, which indicates that the development of MSZ is related to the degree of undercooling. In the study of Caironi et al. (2000), zircon grains were found in a chilled monzogranite in the form of an elongated core with enrichments in Y, Th and U, and are considered to be a consequence of local non-equilibrium conditions due to rapid cooling.

Based on the crystallization order of MSZ overgrown on ESZ, ESZ may be deduced as being formed in a deep magma chamber (i.e., before magma ascent). Generally speaking, the growth rate of zircon in a magma chamber was significantly lower than the diffusion rate of its constituent elements due to slowly decreasing temperature, and the constituent elements with larger ionic radii (U, Th, and Y, etc.) will tend to be excluded from the zircon lattice, due to their partition coefficients being 2 – 3 orders of magnitude lower than that of Zr (Mahood and Hildreth, 1983). In fact, besides its structural and chemical homogeneity, ESZ is characterized by depletion of the elements with larger ionic radii, and thus it may be considered to have formed under close-to-equilibrium conditions (Vavra et al., 1999; Fowler et al., 2002), and probably in a magma chamber from a silicate melt (Hanchar and Miller, 1993; Alexandrov et al., 2000). On the other hand, it is often observed that some euhedral zircon grains contain magma crystallizing mineral inclusions such as apatite and Fe-Ti oxides in porphyritic

lavas, and they were indeed formed in a magma chamber (Fukuoka and Kigoshi, 1974; Sparks et al., 1984; Marsh and Maxey, 1985; Reid et al., 1997; Charlier and Zellmer, 2000); more directly, zircon grains have been separated from volcanic glass (Poldervaart, 1956). Recently, an ion-microprobe study of some rhyolites inferred that the zircon grains crystallized before eruption (Reid et al., 1997).

Similarly, based on the crystallization order of LSZ overgrown on MSZ, LSZ may be deduced as being formed in the emplacement site (i.e., after magma ascent). In fact, since the temperature of a magma in an emplacement site decreases faster than in a deep magma chamber, but less fast than in an ascent passage, the crystallization environment of LSZ should be intermediate between equilibrium as for ESZ and non-equilibrium as for MSZ. This may be reflected by the chemistry of the zircons (i.e., linear variation between U and Th with lower Th/U ratios < 1) and the specific structure (i.e., oscillatory zoning), which is said to be self-organized and formed under far-from-equilibrium conditions (Fowler et al., 2002). On the other hand, very high contents of the substituent elements with larger ionic radii (i.e., U, Th, Y) in LSZ would indicate a double effect: supercooling and fractional crystallization of rock-forming minerals, which correspond probably to crystallization in the supercrust where the magma has just been emplaced.

Recent studies show that the rapid growth under non-equilibrium conditions results in selective substitution of trace elements on different faces (Sunagawa, 1987; Benisek and Finger, 1993). Trace elements with larger ionic radii (i. e., U, Th, Y and REE) are situated preferably on the {101} pyramid faces (Fielding, 1970; Speer, 1982; Carpéna et al., 1987; Vavra, 1990, 1994; Wang and Kienast, 1999; Wang, X. et al., 2002), and on the {110} prism faces (Carpéna et al., 1987; Klötzli, 1999), creating crystals with the {101}- and {110}-dominated typology (corresponding to greater values of I_{py} and I_{pr}) due to the growth blocking effect of the trace elements on these two faces (Benisek and Finger, 1993; Klötzli, 1999). In contrast, ESZ is characterized by chemical "purity" due to its crystallization under near-equilibrium conditions; in this case the development of the {100} and the {211} faces was little constrained, resulting in the dispersive values of I_{py} and I_{pr}. In fact, the typology of ESZ is similar to theoretical form of zircon under equilibrium conditions (Wang and Zhou, 2001). This typological evolutionary progression (i.e., increasing I_{py} and I_{pr} from ESZ to LSZ) is very common in magmatic rocks, as reported by Vavra (1993), Vavra (1994) and Wang and Kienast (1999).

It has been emphasized that the steep increase in trace elements (Hf, U, Th and Y) from the inner band to the outer rim suggests a consequence of enrichment in Hf, U and Y in the granitic melt through fractional crystallization (Exley, 1980; Speer, 1982; Sawka, 1988; Pupin, 1992; Halden et al., 1993; Benisek and Finger, 1993; Watson, 1996; Caironi et al., 2000), because all three elements are incompatible in the granitic melt (Exley, 1980; Speer, 1982; Wark and Miller, 1993). However, no line of evidence has been provided in the literature to prove that LSZ crystallized from the residual magma. In contrast, our research reveals a nearly continuous growth from MSZ to LSZ without any resorption of MSZ (i.e., MSZ shows euhedral contour) before LSZ growth. In fact, LSZ in both the gabbro and the granite from the Pingtan magmatic complex is basically included within the primary rock-forming minerals (biotite, plagioclase, K-feldspar, quartz, etc.), and does not occur as interstitial grains between the rock-forming minerals. Therefore, they crystallized at the beginning of magma consolidation just after magma ascent.

Both the Pingtan magmatic complex gabbro and granite, although they are distinct in chemical composition, show many similarities in typological, structural and geochemical evolution from ESZ via MSZ to LSZ due to their identical physical processes during the complete magmatic activity: ESZ, MSZ and LSZ represent crystallization in a deep magma chamber, in the ascent passage of a magma, and LSZ in an emplacement location of the magma, respectively.

4.3 Implications for geochronology

According to classical ideas, zircon crystallizes in residual basaltic magma since the magma would have been saturated in ZrO_2 and SiO_2 only after fractional crystallization of the majority of rock-forming minerals (Poldervaart, 1956; Konzett et al., 1998; Vavra et al., 1999), and it, as a liquidus phase, crystallized before any of the other minerals in the granitic magma (Poldervaart, 1956; Alper and Poldervaart, 1957; Larsen and Poldervaart, 1957). However, our studies reveal that a population of zircons in magmatic rocks, whether basic or acid, may be composed of three stages of zircon: ESZ, MSZ and LSZ. Because MSZ is least developed, the zircon population of magmatic origin was generally divided into two groups: 'early' vs. 'late' (Krasnobayev, 1979; Volpe and Hammond, 1991; Bourdon et al., 1994; Charlier and Zellmer, 2000). Both were also cited as "colorless and transparent" vs. "colored and semi-transparent" (Krasnobayev, 1979), "common or crystalline" vs. "metamict" (Bogolomov, 1991; Cherniak et al., 1991; Lee et al., 1997), "clear" vs. "clouded" (Brindley and Gupta, 1973), and "core" vs. "rim"' from polished sections of grains (Krasnobayev, 1979; Exley, 1980; Ansdell and Kyser, 1991; Gebauer and Grunenfelder, 1979), respectively.

Zircon has proved to be by far the most useful mineral for U/Pb geochronology because, in addition to an extremely high ratio of U to the initial common Pb, it is mechanically and chemically inert. U/Pb zircon ages are now a staple in integrated tectonic and petrologic investigations, providing age constraints for magmatic events. In actual zircon U-Pb dating, a magmatic rock was commonly considered to have only one age, representing the emplacement age or the crystallization age of the host magma. Thus, when two groups of U-Pb ages with not too large an interval and good concordance have been produced in a magmatic rock, the "appropriate" one is adopted and another is abandoned although two groups of zircon have been observed and distinguished during U-Pb dating. In this case two explanations were presented by: 1) taking the younger age from the euhedral rims as the crystallizing age of the magmatic rock, and the older age from the cores as the age of the source materials (Roddick and Bevier, 1995; Da Silva et al., 2000), or 2) taking the older age from the euhedral cores as the crystallizing age of the magmatic rock, and the younger age from the rims as the age of a subsequent hydrothermal or metamorphic event (Nemchin and Pidgeon, 1997; Guan et al., 1998; Da Silva et al., 2000).

Geochronological data reported in the literature show that zircon grains in magmatic rocks often give two groups of concordant ages (marked as A type in Table 3), or a large range of concordant ages (marked as B type in Table 3). Whether the former or the latter, the intervals reach several tens of Ma! So large spans of time greatly exceed, on one hand, the analytical error (2σ) from the above methods of zircon U-Pb dating, which is only in the order of several Ma, and on the other hand, the time of magma consolidation at the emplacement site, which is generally considered to be less than 10 Ma (Paterson and Tobisch, 1992; Keay et al., 1999). Consequently, there exist effectively at least two stages of zircon or a long-lived crystallization of zircon in a single granitic magmatism. Combining our observations and previous results, this paper considers that such large spans of time would be derived from the difference in crystallization time between ESZ and LSZ. There are four lines of evidence to support this consideration:

(1) Objectively, ESZ occurs essentially as single crystals without overgrowth of MSZ and LSZ (Fig. 2a–c, 2f, 2g), indicating that they stopped growing earlier because of being included within the rock-forming minerals in the magma chamber. A more recent ion-microprobe study of younger rhyolites infers that the zircon grains crystallized before eruption (Reid et al., 1997);

(2) In the literature we have found a negative-correlation between zircon U-Pb ages and U content in zircons from magmatic rocks (Vavra et al., 1999; Da Silva et al., 2000; Yang et al., 2001; Wang Yong et al., 2002), indicating probably that U-enriched grains (i.e., LSZ) are commonly younger than U-depleted grains (i.e., ESZ);

(3) From the literature the total-rock Rb-Sr ages may be much smaller than zircon U-Pb ages (the interval may reach up to about 80 Ma) in magmatic rocks (Williams et al., 1983; Schärer et al., 1986; Alexandrov et al., 2000; Wu et al., 2003), indicating a possibility that zircon may have stopped crystallizing before the magma ascent (Williams et al., 1983), i.e., ESZ may have much older ages than that of magma consolidation at lower closure temperature of a Rb-Sr system;

(4) Pitcher (1978) found that the magmatism of continental margins is characterized by its persistence in time. For example, many successive intrusions of the Coastal Batholith of Peru were emplaced over a period of about 70 Ma. Although the crust is capable of yielding a considerable quantity of acid magma, its ability to provide further batches of magma is greatly diminished after a substantial episode of partial melting. Thus, the above phenomena could be responsible for a pulsant intrusion from the same magma chamber with a long residual time.

The magmatism generally includes two main processes: partial melting at depth and magma consolidation at the emplacement site. It is assumed that the magma at the emplacement site would be solidified in a relatively short period (Paterson and Tobisch, 1992; Keay et al., 1999), which means that the ages of LSZ could represent the time of magma consolidation, just after magma ascent. Consequently, the ages of ESZ would represent the residual time of the magma chamber, just after partial melting. The difference in age between ESZ and LSZ is called in this paper the "rock-forming difference in age" of magmatic rocks, representing the time span of a single magmatism.

If "rock-forming difference in age" for magmatic rocks is indeed large enough by several tens of Ma, then an interesting question follows: what is the petrogenetic implication at a tectonic scale? Generally speaking, magma ascent and emplacement are related more or less to extensional regime (Pitcher, 1979), but magma generation by partial melting at depth may be caused by different tectonic mechanisms. For example, the partial melting of crustal rocks can be generated through crustal thickening in a continental orogenic belt (De Yoreo, 1988; Hutton and Reavy, 1992; D'Lemos et al., 1992), but also through crustal thinning in continental rift zones (Almont, 1986). Evidently, the rates of melting, emplacing and cooling for magmatic rocks would vary with their tectonic regime, and these may be constrained quantitatively by the "rock-forming difference in age" as a future objective of petrogenesis of magmatic rocks.

Table 3 Synthesis of data on concordant $^{206}Pb/^{238}U$ ages of zircons using the SHRIMP or TIMS methods

No.	Rock	Age (Ma)		Method	Reference
A		ESZ	LSZ		
1	Gabbro	317±4	261±12 (*n*=9)	SHRIMP	Vavra et al. (1999)
2	Intermediate igneous rock	343.9±9.5 (n=9)	288±16 (*n*=5)	SHRIMP	Vavra et al. (1999)
3	Diorite	181.7±2.8	127±5.5	TIMS	Li et al. (1999)
4	Adamellite	443.1±2.2 (n=9)	422.0±1.5 (*n*=22)	SHRIMP	Keay et al. (1999)
5	Granite	388±5	367.8±3.0 (*n*=2)	SHRIMP	Kröner et al. (2000)
6	Granite	495.5±3.8 (n=5)	419.9±1.7 (*n*=14)	SHRIMP	Keay et al. (1999)
7	Granite	497±5 (n=15)	474±2 (*n*=2)	SHRIMP	Wilde et al. (2003)
8	Granite	612±8, 627±8	547±6 (*n*=17)	SHRIMP	Da Silva et al. (2000)
B		Zircon Population			
1	Peridotite	300±3 – 262±2 (n=5)		SHRIMP	Vavra et al. (1999)
2	Pyroxenite	159.6±1.3 – 134.7±0.9 (*n*=10)		SHRIMP	Chen et al. (2001)
3	Pyroxenite	158±4 – 97±3 (n=7)		SHRIMP	Liu et al. (2004)
4	Leuconorite	631.5±1.0 – 548.7±3.2 (*n*=33)		SHRIMP	Ashwal et al. (1999)
5	Diorite	395.5±7.5 – 361.8±6.8 (*n*=14)		SHRIMP	Muir et al. (1996)
6	Granite	409±9 – 370±8 (*n*=31)		SHRIMP	Elburg (1996)
7	Granite	155±3 – 121±2 (*n*=20)		SHRIMP	Guan et al. (1998)
8	Granite	411±6 – 379±7 (*n*=12)		SHRIMP	Wu et al. (2004)
9	Granite	395.5±5.1 – 366.4±5.7 (*n*=21)		SHRIMP	Muir et al. (1996)
10	Granite	413.6±20.2 – 359.5±17.5 (*n*=19)		SHRIMP	Muir et al. (1996)
11	Leucogranite	417±11 – 365±10 (*n*=24)		SHRIMP	Elburg (1996)
12	Granophyre	133±0.8 – 106±0.4 (*n*=5)		TIMS	Wang Yong et al. (2002)
13	Adamellite	450 – 400 (*n*=25)		SHRIMP	Keay et al. (1999)
14	Granite	218.8 – 160.1 (*n*=6)		TIMS	Yang et al. (2001)
15	Granite	486 – 424 (*n*=15)		SHRIMP	Roddick and Bevier (1995)
16	Granite	436 – 373 (*n*=15)		SHRIMP	Roddick and Bevier (1995)

5 Conclusions

The determination of multi-stages of zircon growth in magmatic rocks is critical to our estimation of physical conditions during their formation and to any estimation of the length of the zircon crystallization period as a formation process of the host rock, including the generation, ascent and consolidation of the magma.

Our research on morphology and chemistry of zircons demonstrates that zircon growth in both the gabbro and the granite of the Pingtan magmatic complex can be divided into three stages: ESZ (colorless, high transparence and birefringence, low and dispersive I_{pr} and I_{py}, weak and homogeneous BSE brightness, lower Hf contents and deplation of U, Th and Y), MSZ (abruptly increasing I_{py}, progressively strong and sectoral-zoning BSE brightness, higher Hf contents and enrichment of U, Th and Y with Th/U > 1), and LSZ (brownish, low transparence and birefringence, highest I_{pr} and I_{py}, middle and oscillatory-zoned BSE brightness, highest contents of Hf, U and Y with Th/U < 1). According to the above petrogenetic characters three stages of zircon growth are considered to have formed in a deep magma chamber, ascent passage and emplacement site, respectively. This correlation is very important not only for revealing the physical conditions of each stage of crystallization, but also for revealing the chemical effect on Zr, Hf, U, Th and REE distributions, which are generally considered to be incompatible during fractional crystallization.

On the other hand, many results in the literature of precise U-Pb dating of zircons often show two groups of concordant ages or a large range of concordant ages, whether the former or latter, the intervals reach several tens of Ma. So here large spans of time are considered to be represented by the difference in crystallization time between ESZ and LSZ, which may be attributed to the tectonic constraints for the magmatism.

Acknowledgements

This work is supported by the National Natural Science Foundation of China (No. 40572038).

Manuscript received Aug. 8, 2005
accepted April 10, 2006
edited by Xie Guanglian and Susan Turner

References

Alexandrov, P., Cheilletz, A., Deloule, E., and Cuney, M., 2000. 319±7 Ma crystallization age for the Blond granite (northwest Limousin, French Massif Central) obtained by U/Pb ion-probe dating of zircons. *Comptes Rendus de l'Academie des Sciences Series IIA, Earth and Planetary Science*, 330: 617–622.

Almont, D.C., 1986. Geological evolution of the Afro-Arabian dome. *Tectonophysics*, 131: 301–332.

Alper, A.M., and Poldervaart, A., 1957. Zircons from the Animas Stock and associated rocks, Mexico. *Econ. Geol.*, 52: 952–971.

Ansdell, K.M., and Kyser, T.K., 1991. Plutonism, deformation, and metamorphisms in the Proterozoic Flin Flon greenstone belt, Canada; limits on timing provided by the single-zircon Pb-evaporation technique. *Geology*, 19: 518–521.

Ashwal, L.D., Tucker, R.D., and Zinner, E.K., 1999. Slow cooling of deep crustal granulite and Pb-loss zircon. *Geochim. Cosmochim. Acta*, 63: 2839–2851.

Belousova, E.A., Griffin, W.L., O'Reilly, S.Y., and Fisher, N.I., 2002. Trace elements in zircon: Relationship to source rock type. *Contrib. Mineral. Petrol.*, 143: 602–622.

Benisek, A., and Finger, F., 1993. Factors controlling the development of prism faces in granite zircons: a microprobe study. *Contrib. Mineral. Petrol.*, 114: 441–451.

Bogolomov, Y.S., 1991. Migration of lead in non-metamict zircon. *Earth Planet. Sci. Lett.*, 107: 625–633.

Bourdon, B., Zindler, A., and Wörner, G., 1994. Evolution of the Laacher See magma chamber: evidence from SIMS and TIMS measurements of U-Th disequilibria in minerals and glasses. *Earth Planet. Sci. Lett.*, 126: 75–90.

Brindley, J.C., and Gupta, L.N., 1973. History of zircon growth from minor acid intrusions in south east Ireland. *Scientific Proceedings of the Royal Dublin Society*, A4: 411–430.

Broska, I., Bibikova, E., Gracheva, T., Makarov, V., and Cano, F., 1990. Zircon from granitoid rocks of the Tribec-Zobor crystalline complex; its typology, chemical and isotopic composition. *Geologica-Carpathica*, 41: 393–406.

Bryan, W.B., 1972. Morphology of quench crystals in submarine basalts. *J. Geophys. Res.*, 77: 5812–5819.

Burton, J.A, Prim, R.C., and Slichter, W.P., 1953. The distribution of solute in crystals grown from the melt. Part I. Theoretical. *J. Chem. Phys.*, 21: 1987–1991.

Caironi, V., Colombo, A., Tunesi, A., and Gritti, C., 2000. Chemical variations of zircon compared with morphological evolution during magmatic crystallization: an example from the Valle del Cervo Pluton (Western Alps). *Europ. J. Mineral.*, 12: 779–794.

Carpéna, J., Gagnol, I., Mailhé, D., and Pupin, J.P., 1987. L'uranium marqueur de la croissance cristalline: mise en évidence par les traces de fission dans les zircons gemmes d'Espaly (Haute-Loire, France). *Bull. Minéral.*, 110: 459–463.

Charlier, B., and Zellmer, G., 2000. Some remarks on U-Th mineral ages from igneous rocks with prolonged crystallization histories. *Earth Planet. Sci. Lett.*, 183: 457–469.

Chen Daogong, Wang Xiang, Deloule, E., Li Binxian, Xia Qunke, Cheng Hao, and Wu Yuanbao, 2001. Zircon SIMS ages and chemical compositions from Northern Dabie Terrain: Its implication for pyroxenite genesis. *Chinese Sci. Bull.*, 46: 1047–1050.

Cherniak, D.J., Lanford, W.A., and Ryerson, F.J., 1991. Lead diffusion in apatite and zircon using ion implantation and Rutherford backscattering techniques. *Geochim. Cosmochim. Acta*, 55: 1663–1673.

Connelly, J.N., 2000. Degree of preservation of igneous zonation in zircon as a signpost for concordancy in U/Pb geochronology. *Chem. Geol.*, 172: 25–39.

Corfu, F., 1996. Multistage zircon and titanite growth and inheritance in an Archean gneiss complex, Winnipeg River Subprovince, Ontario. *Earth Planet. Sci. Lett.*, 141: 175–186.

Da Silva, L.C., Gresse, P.G., Scheepers, R., McNaughton, N.J., Hartmann, L.A., and Fletcher, I., 2000. U-Pb SHRIMP and Sm-Nd age constraints on the timing and sources of the Pan-African Cape Granite Suite, South Africa. *J. African Earth Sci.*, 30: 795–815.

De Yoreo, J.J., 1988. Thermal models for granite genesis following crustal thickening. *EOS*, 69: 770.

D'Lemos, R.S., Brown, M., and Strachan, R.A., 1992. The relationship between granite and shear zones: magma generation, ascent and emplacement within a transpressional orogen. *J. Geol. Soc. London*, 149: 487–490.

Dong Chuanwan, Zhou Xinmin and Li Huimin, 1997. Late Mesozoic crust/mantle interaction in southeastern Fujian: isotopic evidence from the Pingtan igneous complex. *Chinese Sci. Bull.*, 42: 495–498.

Elburg, M.A., 1996. U-Pb ages and morphologies of zircon in micrograniteoid enclaves and peraluminous host granite: evidence for magma mingling. *Contrib. Mineral. Petrol.*, 123: 177–189.

Exley, R.A., 1980. Microprobe studies of REE-rich accessory minerals: implication for skye granite petrogenesis and REE mobility in hydrothermal systems. *Earth Planet. Sci. Lett.*, 49: 97–110.

Faure, G., 1977. *Principals of Isotope Geology*. New York: John Wiley and Sons, 464.

Fielding, P.E., 1970. The distribution of uranium, rare earths, and color centers in a crystal of natural zircon. *Am. Mineral.*, 55: 428–440.

Fowler, A., Prokoph, A., Stern, R., and Dupuis, C., 2002. Organization of oscillatory zoning in zircon: Analysis, scaling, geochemistry, and model of a zircon from Kipawa, Quebec, Canada. *Geochim. Cosmochim. Acta*, 66: 311–328.

Fukuoka, T., and Kigoshi, K., 1974. Discordant Io-ages and the uranium and thorium distribution between zircon and host rocks. *Geochem. J.*, 8: 117–122.

Gebauer, D., and Grunenfelder, M., 1979. U-Pb zircon and Rb-Sr mineral dating of eclogites and their country rocks, Munchberg gneiss massif, NE Bavaria. *Earth Planet. Sci. Lett.*, 42: 35–44.

Guan Kuang, Luo Zhenkuan, Miao Leicheng and Huang Jiazhan, 1998. SHRIMP in zircon chronology for Guojialing suite granite in Jiaodong Zhaoye district. *Scientia Geologica Sinica*, 33: 318–328 (in Chinese with English abstract).

Guo, J., O'Reilly, S.Y., and Griffin, W.L., 1996. Zircon inclusions in corundum megacrysts: I. Trace element geochemistry and clues to the origin of corundum megacrysts in alkali basalts. *Geochim. Cosmochim. Acta*, 60: 2347–2363.

Halden, N.M., Hawthorne, F. C., Campbell, J. L., Teesdale, W. J., Maxwell, J. A., and Higuchi, D., 1993. Chemical characterization of oscillatory zoning and overgrowths in zircon using 3 MeV μ-pixe. *Can. Mineral.*, 31: 637–647.

Hanchar, J.M., and Miller, C.F., 1993. Zircon zonation patterns as revealed by cathodoluminescence and backscattered electron images: Implications for interpretation of complex crustal histories. *Chem. Geol.*, 110: 1–13.

Hutton, D.H.W., and Reavy, R.J., 1992. Strike-slip tectonics and granite petrogenesis. *Tectonics*, 11: 960–967.

Keay, S., Steele, D., and Compston, W., 1999. Identifying granite sources by SHRIMP U-Pb zircon geochronology: an application to the Lachlan foldbelt. *Contrib. Mineral. Petrol.*, 137: 323–341.

Klötzli, U.S., 1999. Th/U zonation in zircon derived from evaporation analysis: a model and its implications. *Chem. Geol.*, 158: 325–333.

Krasnobayev, A.A., 1979. Mineralogical-geochemical features of zircons from kimberlites and problems of their origin. *Intl. Geol. Rev.*, 22: 1199–1209.

Konzett, J., Armstrong, R.A., Sweeney, R.J., and Compston, W., 1998. The timing of MARID metasomatism in the Kaapvaal

mantle: an ion probe study of zircons from MARID xenoliths. *Earth Planet. Sci. Lett.*, 160: 133–145.

Kröner, A., Jaeckel, P., and Brandl, G., 2000. Single zircon ages for felsic to intermediate rocks from the Pietersburg and Giyani greenstone belts and bordering granitoid orthogneisses, northern Kaapvaal Craton, South Africa. *J. African Earth Sci.*, 30: 773–793.

Larsen, L.H., and Poldervaart, A., 1957. Measurement and distribution of zircons in some granitic rocks of magmatic origin. *Mineral. Mag.*, 31, 544–564.

Lee, J.K.W., Williams, I.S., and Ellis, D., 1997. Pb, U and Th diffusion in natural zircon. *Nature*, 390: 159–162.

Li Shuguang, Hong Ji-an, Li Huimin and Jiang Leili, 1999. Zircon U-Pb age of gabbro-pyroxenite complex from Dabie mountains and its geological implication. *Geol. J. China Univ.*, 5: 351–355 (in Chinese with English abstract).

Liu Yongsheng, Yuan Honglin, Gao Shan, Hu Zhaochu, Wang Xuance, Liu Xiaoming and Lin Wenli, 2004. Zircon U-Pb ages of olive pyroxenite xenolith from Hannuoba: links between the 97-158 Ma basaltic underplating and granulite-facies metamorphism. *Chinese Sci. Bull.*, 49: 1055–1062.

Mahood, G., and Hildreth, W., 1983. Large partition coefficient for trace elements in high-silica rhyolites. *Geochim. Cosmochim. Acta*, 47: 11–30.

Marsh, B.D., and Maxey, M.R., 1985. On the distribution and separation of crystals in convection magma. *J. Volcanol. Geothermal Res.*, 24: 95–150.

Muir, R.J., Ireland, T.R., Weaver, S.D., and Bradshaw, J.D., 1996. Ion microprobe dating of Paleozoic granitoids: Devonian magmatism in New Zealand and correlations with Australia and Antarctica. *Chem. Geol.*, 127: 191–210.

Nasdala, L., Wenzel, T., Pidgeon, R.T., and Kronz, A., 1999. Internal structures and dating of complex zircons from Meissen Massif monzonites, Saxony. *Chem. Geol.*, 156: 331–341.

Nemchin, A.A., and Pidgeon, R.T., 1997. Evolution of the Darling Range Batholith, Yilgarn Craton, Western Australia: a SHRIMP zircon study. *J. Petrol.*, 38: 625–649.

Paterson, B.A., Stephens, W.E., Rogers, G., Williams, I.S., Hinton, R.W., and Herd, D.A., 1992. The nature of zircon inheritance in two granite plutons. *Trans. Royal Soc. Edinburgh: Earth Sci.*, 83: 459–471.

Paterson, S.R., and Tobisch, O.T., 1992. Rates of processes in magmatic arcs: Implications for the timing and nature of pluton emplacement and wall rock deformation. *J. Struct. Geol.*, 14, 291–300.

Pidgeon, R.T., and Compston, W., 1992. A SHRIMP ion microprobe study of inherited and magmatic zircons from four Scottish Caledonian granites. *Trans. Royal Soc. Edinburgh: Earth Sci.*, 83: 473–483.

Pitcher, W.S., 1978. The anatomy of a batholith. *J. Geol. Soc. London*, 135: 157–182.

Pitcher, W.S., 1979. The nature, ascent and emplacement of granitic magmas. *J. Geol. Soc. London*, 136: 627–662.

Poitrasson, F, Paquette, J.L., Montel, J.M., Pin, C., and Duthou, J. L., 1998. Importance of late-magmatic and hydrothermal fluids on the Sm-Nd isotope mineral systematics of hypersolvus granites. *Chem. Geol.*, 146: 187–203.

Poldervaart, A., 1956. Zircons in rocks. 2. Igneous rocks. *Am. J. Sci.*, 254: 521–554.

Pupin, J.P., 1992. Les zircons des granites océaniques et continentaux: couplage typologie - géochemie des éléments en traces. *Bull. Soc. Géol. France*, 163: 495–507.

Pupin, J.P., 2000. Granite genesis related to geodynamics from Hf-Y in zircon. *Trans. Royal Soc. Edinburgh: Earth Sci.*, 91: 245–256.

Reid, M.R., Coath, C.D., Harrison, T.M., and McKeegan, K.D., 1997. Prolonged residence times for the youngest rhyolites associated with Long Valley Caldera: ^{230}Th-^{238}U ion microprobe dating of young zircons. *Earth Planet. Sci. Lett.*, 150: 27–39.

Roddick, J.C., and Bevier, M.L., 1995. U-Pb dating of granites with inherited zircon: Conventional and ion microprobe results from two Paleozoic plutons, Canadian Appalachians. *Chem. Geol.*, 119: 307–329.

Rubin, J.N., Henry, C.D., and Price, J.G., 1989. Hydrothermal zircon at zircon overgrowths, Sierra Blanca Peaks, Texas. *Am. Mineral.*, 74: 865–869.

Sawka, W.N., 1988. REE and trace element variations in accessory minerals and hornblende from the strongly zoned McMurry Meadows Pluton, California. *Trans. Royal Soc. Edinburgh: Earth Sci.*, 79: 157–168.

Schärer, U., Xu, R.H., and Allegre, C.J., 1986. U-(Th)-Pb systematics and ages of Himalayan leucogranites, South Tibet. *Earth Planet. Sci. Lett.*, 77: 35–48.

Schärer, U., Zhang, L.S., and Tapponnier, O., 1994. Duration of strike slip movements in large shear zones: The Red River belt, China. *Earth Planet. Sci. Lett.*, 126: 379–397.

Silver, L.T., and Deutsch, S., 1963. Uranium-lead isotopic variations in zircons: a case study. *J. Geol.*, 71: 721–758.

Sparks, R.S.J., Huppert, H.E., and Turner, J.S., 1984. The fluid dynamics of evolving magma chambers. *Phil. Trans. Royal Soc. London*, 310: 511–534.

Speer, J.A., 1982. Zircon. In: Ribbe, P.H. (ed.), Orthosilicates. *Rev. Mineral.*, 5: 67–112.

Sunagawa, I., 1987. Morphology of minerals. In: Sunagawa, I. (ed.), *Morphology of Crystals*, Tokyo: Terra Science Publication Company, 63–105.

Vavra, G., 1990. On the kinematics of zircon growth and its petrogenetic significance: a cathodoluminescence study. *Contrib. Mineral. Petrol.*, 106: 90–99.

Vavra, G., 1993. A guide to quantitative morphology of accessory zircon. *Chem. Geol.*, 93: 15–28.

Vavra, G., 1994. Systematics of internal zircon morphology in major Variscan granitoid types. *Contrib. Mineral. Petrol.*, 117: 331–344.

Vavra, G., Schmid, R., and Gebauer, D., 1999. Internal morphology, habit and U-Th-Pb microanalysis of amphibolite-to-granulite facies zircons: geochronology of the Ivrea Zone (southern Alps). *Contrib. Mineral. Petrol.*, 134: 380–404.

Veniale, F., Pigorini, B., and Soggetti, F., 1968. Petrological significance of the accessory zircon in the granites from Baveno, M. Orfano and Alzo (North Italy). *23th Intl. Geol. Congr.*, 13: 243–268.

Volpe, A.M., and Hammond, P.E., 1991. ^{238}U-^{230}Th-^{236}Ra disequilibria in young Mount St. Helens rocks: time constraint for magma formation and crystallization. *Earth Planet. Sci. Lett.*, 107: 475–486.

Wang Xiang, 1998. Quantitative description of zircon morphology and its dynamics analysis. *Sci. China* (D), 41: 422–428.

Wang Xiang and Kienast, J.R., 1999. Morphology and geochemistry of zircon: a case study on zircon from the

microgranitoid enclaves. *Sci. China* (D), 42: 544–552.

Wang Xiang and Zhou Dongshan, 2001. A new equilibrium form of zircon crystal. *Sci. China* (B), 44: 516–522.

Wang Xiang and Li Wuxiang, 2002. Typomorphism of the {211}-type zircon. *Chinese Sci. Bull.*, 47: 154–158.

Wang, X., Griffin, W.L., O'Reilly, S.Y., Zhou, X.M., Xu, X.S., Jackson, S.E., and Pearson, N.J., 2002. Morphology and geochemistry of zircons from late Mesozoic igneous complexes in coastal SE China: implications for petrogenesis. *Mineral. Mag.*, 66: 235–251.

Wang Yong, Guan Taiyang, Huang Guofu, Yu Daxin and Chen Conglin, 2002. Isotope chronological studies of late Yanshanian volcanic rocks in northeast Jiangxi Province. *Acta Geoscientia Sinica*, 23: 233–236 (in Chinese with English abstract).

Wark, D.A., and Miller, C.F., 1993. Accessory mineral behavior during differentiation of a granite suite: monazite, xenotime and zircon in the Sweetwater Wash pluton, southeastern California, U.S.A. *Chem. Geol.*, 110: 49–67.

Watson, E.B., 1996. Dissolution, growth and survival of zircons during crustal fusion: kinetic principles, geological models and implications for isotopic inheritance. *Trans. Royal Soc. Edinburgh: Earth Sci.*, 87: 43–56.

Wilde, S.A., Wu, F.Y., and Zhang, X.Z., 2003. Late Pan-African magmatism in northeastern China: SHRIMP U-Pb zircon evidence from granitoids in the Jiamusi Massif. *Precambrian Res.*, 122: 311–327.

Williams, I.S., 1992. Some observations on the use of zircon U-Pb geochronology in the study of granitic rocks. *Trans. Royal Soc. Edinburgh: Earth Sci.*, 83: 447–458.

Williams, I.S., Compston, W., and Chappell, B.W., 1983. Zircon and monazite U-Pb systems and the histories of I-type magmas, Berridale Batholith, Australia. *J.Petrol.*, 24: 76–97.

Wu, F.Y, Jahn, B.M., Wilde, S.A., Lo, C.H., Yui, T.F., Lin, Q., and Ge, W.C., 2003. Highly fractionated I-type granites in NE China (I): geochronology and petrogenesis. *Lithos*, 66: 241–273.

Wu Cailai, Yang Jingshui, Wooden, J.L., Shi Rendeng, Chen Songyong, Meibom, A., and Mattinson, C., 2004. Zircon U-Pb SHRIMP dating of the Yematan batholith in Dulan, North Qaidam, NW China. *Chinese Sci. Bull.*, 49: 1736–1740.

Xu, X.S., Dong, C.W., Li, W.X., and Zhou, X.M., 1999. Late Mesozoic intrusive complexes in the coastal area of Fujian, SE China: the significance of the gabbro-diorite-granite association. *Lithos*, 46: 299–315.

Yang Fuquan, Wang Liben, Ye Jinhua, Fu Xuji and Li Huimin, 2001. Zircon U-Pb ages of granites in the Huoshi Bulak area, Xinjiang. *Regional Geol. China*, 20: 267–273 (in Chinese with English abstract).

Yeliseyeva, O.P., Ryabchikov, I.D., and Bogatyreva, N.A., 1974. On the types of distribution of uranium in accessory zircon. *Geochem. Intl.*, 11: 960–967.

Zartman, R.E., and Hermes, O.D., 1987. Archean inheritance in zircon from late Paleozoic granites from the Avalon zone of southeastern New England: an African connection. *Earth Planet. Sci. Lett.*, 82: 305–315.

Zeck, H.P., and Whitehouse, M.J., 2002. Repeated age resetting in zircons from Hercynian-Alpine Polymetamorphic schists (Betic-Rif tectonic belt, S. Spain): a U-Th-Pb ion microprobe study. *Chem. Geol.*, 182: 275–292.